High-density carbon ablator experiments on the National Ignition Facilitya)

A. J. MacKinnon, N. B. Meezan, J. S. Ross, S. Le Pape, L. Berzak Hopkins, L. Divol, D. Ho, J. Milovich, A. Pak, J. Ralph, T. Döppner, P. K. Patel, C. Thomas, R. Tommasini, S. Haan, A. G. MacPhee, J. McNaney, J. Caggiano, R. Hatarik, R. Bionta, T. Ma, B. Spears, J. R. Rygg, L. R. Benedetti, R. P. J. Town, D. K. Bradley, E. L. Dewald, D. Fittinghoff, O. S. Jones, H. R. Robey, J. D. Moody, S. Khan, D. A. Callahan, A. Hamza, J. Biener, P. M. Celliers, D. G. Braun, D. J. Erskine, S. T. Prisbrey, R. J. Wallace, B. Kozioziemski, R. Dylla-Spears, J. Sater, G. Collins, E. Storm, W. Hsing, O. Landen, J. L. Atherton, J. D. Lindl, M. J. Edwards, J. A. Frenje, M. Gatu-Johnson, C. K. Li, R. Petrasso, H. Rinderknecht, M. Rosenberg, F. H. Séguin, A. Zylstra, J. P. Knauer, G. Grim, N. Guler, F. Merrill, R. Olson, G. A. Kyrala, J. D. Kilkenny, A. Nikroo, K. Moreno, D. E. Hoover, C. Wild, and E. Werner

Citation: Physics of Plasmas (1994-present) **21**, 056318 (2014); doi: 10.1063/1.4876611
View online: http://dx.doi.org/10.1063/1.4876611
View Table of Contents: http://scitation.aip.org/content/aip/journal/pop/21/5?ver=pdfcov
Published by the AIP Publishing

Articles you may be interested in

The high-foot implosion campaign on the National Ignition Facilitya)
Phys. Plasmas **21**, 056314 (2014); 10.1063/1.4874330

Hydrodynamic instability growth and mix experiments at the National Ignition Facilitya)
Phys. Plasmas **21**, 056301 (2014); 10.1063/1.4872026

Cryogenic thermonuclear fuel implosions on the National Ignition Facilitya)
Phys. Plasmas **19**, 056318 (2012); 10.1063/1.4719686

A high-resolution integrated model of the National Ignition Campaign cryogenic layered experimentsa)
Phys. Plasmas **19**, 056315 (2012); 10.1063/1.4718595

Simulation and design study of cryogenic cone shell target for Fast Ignition Realization Experiment projecta)
Phys. Plasmas **14**, 056303 (2007); 10.1063/1.2671124

This article is copyrighted as indicated in the article. Reuse of AIP content is subject to the terms at: http://scitation.aip.org/termsconditions. Downloaded to IP: 198.125.177.149 On: Wed, 04 Jun 2014 19:38:02

High-density carbon ablator experiments on the National Ignition Facility[a)]

A. J. MacKinnon,[1,b),c)] N. B. Meezan,[1] J. S. Ross,[1] S. Le Pape,[1] L. Berzak Hopkins,[1] L. Divol,[1] D. Ho,[1] J. Milovich,[1] A. Pak,[1] J. Ralph,[1] T. Döppner,[1] P. K. Patel,[1] C. Thomas,[1] R. Tommasini,[1] S. Haan,[1] A. G. MacPhee,[1] J. McNaney,[1] J. Caggiano,[1] R. Hatarik,[1] R. Bionta,[1] T. Ma,[1] B. Spears,[1] J. R. Rygg,[1] L. R. Benedetti,[1] R. P. J. Town,[1] D. K. Bradley,[1] E. L. Dewald,[1] D. Fittinghoff,[1] O. S. Jones,[1] H. R. Robey,[1] J. D. Moody,[1] S. Khan,[1] D. A. Callahan,[1] A. Hamza,[1] J. Biener,[1] P. M. Celliers,[1] D. G. Braun,[1] D. J. Erskine,[1] S. T. Prisbrey,[1] R. J. Wallace,[1] B. Kozioziemski,[1] R. Dylla-Spears,[1] J. Sater,[1] G. Collins,[1] E. Storm,[1] W. Hsing,[1] O. Landen,[1] J. L. Atherton,[1] J. D. Lindl,[1] M. J. Edwards,[1] J. A. Frenje,[2] M. Gatu-Johnson,[2] C. K. Li,[2] R. Petrasso,[2] H. Rinderknecht,[2] M. Rosenberg,[2] F. H. Séguin,[2] A. Zylstra,[2] J. P. Knauer,[3] G. Grim,[4] N. Guler,[4] F. Merrill,[4] R. Olson,[4] G. A. Kyrala,[4] J. D. Kilkenny,[5] A. Nikroo,[5] K. Moreno,[5] D. E. Hoover,[5] C. Wild,[6] and E. Werner[6]

[1]*Lawrence Livermore National Laboratory, P.O. Box 808, Livermore, California 94551-0808, USA*
[2]*Plasma Science and Fusion Center, Massachusetts Institute of Technology, Cambridge, Massachusetts 02139, USA*
[3]*Laboratory for Laser Energetics, University of Rochester, Rochester, New York 14623, USA*
[4]*Los Alamos National Laboratory, Los Alamos, New Mexico 87545, USA*
[5]*General Atomics, P.O. Box 85608, San Diego, California 93286-5608, USA*
[6]*Diamond Materials GmbH, Hans-Bunte-Str. 19, 79108 Freiburg, Germany*

(Received 14 December 2013; accepted 26 March 2014; published online 28 May 2014)

High Density Carbon (HDC) is a leading candidate as an ablator material for Inertial Confinement Fusion (ICF) capsules in x-ray (indirect) drive implosions. HDC has a higher density (3.5 g/cc) than plastic (CH, 1 g/cc), which results in a thinner ablator with a larger inner radius for a given capsule scale. This leads to higher x-ray absorption and shorter laser pulses compared to equivalent CH designs. This paper will describe a series of experiments carried out to examine the feasibility of using HDC as an ablator using both gas filled hohlraums and lower density, near vacuum hohlraums. These experiments have shown that deuterium (DD) and deuterium-tritium gas filled HDC capsules driven by a hohlraum filled with 1.2 mg/cc He gas, produce neutron yields a factor of 2× higher than equivalent CH implosions, representing better than 50% Yield-over-Clean (YoC). In a near vacuum hohlraum (He = 0.03 mg/cc) with 98% laser-to-hohlraum coupling, such a DD gas-filled capsule performed near 1D expectations. A cryogenic layered implosion version was consistent with a fuel velocity = 410 ± 20 km/s with no observed ablator mixing into the hot spot. © *2014 AIP Publishing LLC*. [http://dx.doi.org/10.1063/1.4876611]

I. INTRODUCTION

In the inertial confinement fusion (ICF) hot-spot ignition scheme, kinetic energy from an imploding spherical ablator is converted upon stagnation to internal energy in the fusion fuel hot spot.[1] At the National Ignition Facility (NIF),[2] this is achieved via the indirect-drive method. The fusion capsule consists of a spherical shell of cryogenic deuterium-tritium (DT) fuel surrounded by the ablator. Laser power deposited inside a gold hohlraum is converted to soft x-rays that impinge on the ablator. The ablator material absorbs the x-rays and explodes outward, accelerating the shell and fuel layer inward. In order to achieve a sufficiently high hot spot temperature to initiate thermonuclear burn, the maximum velocity of the cryogenic DT fuel ablator must reach $V_{fuel} \sim 350$ km/s.[3] By the end of the acceleration phase, most (≈90%) of the ablator material surrounding the cryogenic fuel layer has been removed.

Theoretically, to provide the most efficient acceleration, nearly all the ablator material should be removed from the capsule during acceleration—the ablation pressure then acts upon the minimum payload mass.[4] Only a very thin ablator layer is needed to protect the fuel from direct x-ray heating at the end of the implosion. Unfortunately, during the implosion's acceleration phase, the ablation front of the imploding shell is unstable to the Rayleigh-Taylor instability. Although the instability is partially stabilized by the ablation process, it is calculated and observed that defects on the capsule surface grow to several hundred times their original size. It is therefore desirable to keep additional mass between the fuel layer and the ablation front to separate the hotspot from Rayleigh-Taylor growth at the ablation front. On the other hand, increasing the ablator mass of the capsule increases the laser energy and power needed to drive the fuel ablator to the required velocity.

For the NIF baseline ignition capsule design, these two competing design considerations of velocity and remaining ablator mass were balanced using radiation-hydrodynamics simulations and the capsule must achieve a fuel velocity $V_{fuel} = 370$ km/s with $M \geq 0.25$ mg of ablator mass

[a)]Paper YI3 5, Bull. Am. Phys. Soc. **58**, 369 (2013).
[b)]Invited speaker.
[c)]Author to whom correspondence should be addressed. Electronic mail: mackinnon2@llnl.gov

 © 2014 AIP Publishing LLC

This article is copyrighted as indicated in the article. Reuse of AIP content is subject to the terms at: http://scitation.aip.org/termsconditions. Downloaded to IP: 198.125.177.149 On: Wed, 04 Jun 2014 19:38:02

remaining at the time of peak velocity, as described in detail by Meezan *et al.*[5]

In order to maximize compression using the minimum laser energy, the pulse-shape for the "point design" minimizes the entropy of the fuel by using a "low adiabat" pulse-shape. The adiabat, α, is defined as pressure at a given density divided by the Fermi degenerate pressure at a fuel density of 1000 g/cc.[3] For the National Ignition Campaign, a pulse-shape with $\alpha \sim 1.5$ and a CH ablator was used, as described by Edwards *et al.*[6] Experiments using this pulse-shape did produce fuel areal densities within 85% of the point design[7] but neutron yields (10×) and stagnation pressures (3.3×) were significantly lower than the 1D models predicted at the measured implosion velocities. Edwards *et al.*[6] discuss some of the possible reasons for the reduced performance of low adiabat pulses including the effect of low mode hot spot shape, increased sensitivity to hydrodynamic instabilities (HI) at the interfaces between Si doped and undoped CH, larger surface imperfections in the CH ablator and the "tent" fixture that is used to hold the capsule within the hohlraum which could produce enhanced seeds for HI growth. One solution is to use higher adiabat pulse-shapes that reduce fuel compression but are less susceptible to HI instabilities as described by Dittrich.[8] Implosions using these pulse-shapes have indeed shown, in a series of experiments described by Park *et al.*,[9] significantly improved performance close to 1D models.

Alternate ablators such as beryllium and high density carbon (HDC) offer another way of studying the influence of HI on the implosion performance. Both these materials can be fabricated with very smooth surfaces, potentially reducing the seeds for HI.[3] Pure diamond is also useful as it can be used to test the hypothesis of increased HI at doped/undoped interfaces described above.

HDC and Be also have other properties that could make them more attractive for achieving high performance implosions (discussed in detail by Haan *et al.*[3]). The higher density of HDC leads to a thinner initial shell, hence a larger initial inside diameter for the same initial outside diameter, leading to more pdV work done on a larger fuel and hot spot volume. In addition, the thinner shell leads to less absolute inward motion during shock compression such that for the same initial outside diameter, the ablation front is at larger radius when peak of the drive and acceleration begins. This leads to higher efficiency than either CH or Be as the HDC capsules absorbs more energy due to a larger ablation surface area. Nano crystalline HDC, with grain sizes of order 70 nm, can be polished to a very smooth surface, with surface quality much better than (up to factor of 10) the requirements inferred from simulations.[3]

The increased density of HDC also means that there is less shock compression than CH, so that once the shocks transit the ablator the in-flight shell thickness is comparable to or larger than an equivalent CH design.[3] This is an important point because it follows that an initially thinner HDC shell does not lead to an increased sensitivity to HI due to in-flight shell thickness. In addition for a given tolerance δx on the shock merge depth x for ensuring a low fuel adiabat, the thinner initial ablator thickness of HDC vs CH reduces the required merge depth, x. This relaxes the tolerance on the foot laser power accuracy $\delta P_L/P_L \sim 2\delta u_s/u_s \sim 2\delta x/x$ by about 2× (where P_L = laser power, u_s = shock speed).[10] By contrast, in the good approximation that the speed of the first two shocks is similar in ablator as DT ice then the required successive shock launch timing precisions just depend on the relative speeds of the successive shocks.[10]

The higher ablator efficiency and superior surface smoothness of HDC makes it an ideal candidate as an ablator for ignition scale capsules on the NIF, however there is an open question regarding the melting of the diamond during the implosion. Solid or partially melted HDC can provide microstructures that seed HI. Ideally, HDC should be completely melted to achieve spatially uniform shocks. Complete melting requires shock strength of >12 Mbar (Refs. 11 and 12) while the co-existence state requires shock strength >6 Mbar. Recent experiments[13,14] at the Omega facility[15] have shown that keeping diamond in the coexistence regime is sufficient to reduce shock non-uniformities to an acceptable level. This measurement method employs a time-resolved two-dimensional imaging velocity interferometer (VISAR) illuminated by a 2 ps laser pulse, which captures spatial variations in the velocity across the shock front transmitted through the ablator. The measurement is carried out over an 800 μm field of view with relative velocity sensitivity $\delta V/V = 5 \times 10^{-4}$ and over perturbation wavelengths in the range of 4 μm to 50 μm.[13] Data comparing shock uniformity in Be and HDC are shown in Fig. 1. Here, the Omega laser was used to produce a 4.5 Mbar shock in planar samples of Be or HDC. From a qualitative comparison of the 2D velocity uniformity ($\delta V/V$ vs space) maps shown in Fig. 1(a) Be at 3.7 Mbar and (b) HDC at 4.5 Mbar, it is clear that the shock uniformity is very good with Be (which has acceptable uniformity at this shock strength) but is much less uniform with HDC at these shock pressures.

A series of experiments was carried out to determine the shock strength where acceptable uniformity for HDC could be obtained. The results are summarized in Fig. 1(c), which plots the velocity uniformity spectrum for two shock strengths in HDC compared to Be and CH. An increase in the shock strength to 8 Mbar partially melted the HDC leading to dramatically improved shock uniformity (this will be described in detail in a future publication). From these data, it was determined that in order to maintain acceptable shock velocity uniformity the first shock strength should exceed 6 Mbar for all NIF HDC implosion designs. All the pulse shapes described in this paper meet this requirement.

The remainder of this paper is divided into sections: Section II will describe the trade-off between instability growth and the fuel adiabat that determined the current pulse shapes used for HDC experiments on the NIF. Section III will describe the experimental setup. Section IV will describe implosion experiments using low adiabat ($\alpha = 1.5$) 10 ns duration laser pulses to drive HDC capsules in conventional gas filled hohlraums.[16–19] Section V will describe high adiabat ($\alpha = 3.5$) implosion experiments using near vacuum hohlraums for HDC capsules. Section VI will present conclusions and future directions.

This article is copyrighted as indicated in the article. Reuse of AIP content is subject to the terms at: http://scitation.aip.org/termsconditions. Downloaded to IP: 198.125.177.149 On: Wed, 04 Jun 2014 19:38:02

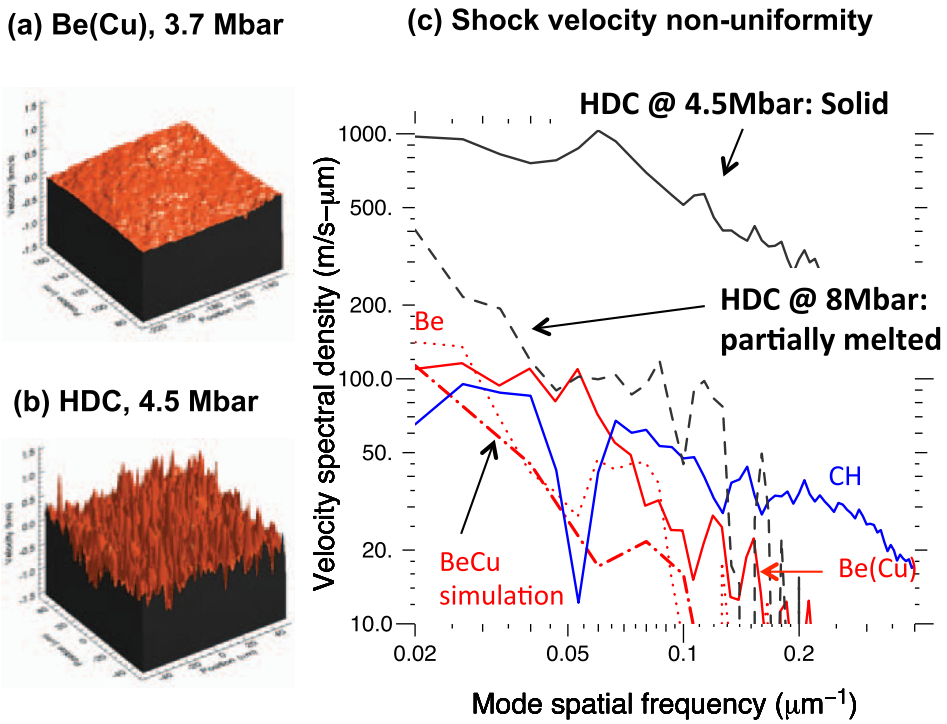

FIG. 1. Experimental results from experiments on the Omega facility showing 2D maps of shock uniformity vs. shock strength for (a) Be and (b) HDC; (c) plots of shock velocity non uniformity for HDC for 4.5 and 8 Mbar shocks vs. CH, Be, and Be(Cu) copper doped beryllium. HDC has acceptable uniformity for shocks >6 Mbar.

II. DESIGN CONSTRAINTS FOR HDC ABLATORS

The most important goals of the HDC campaign on NIF were to determine if there were any fundamental obstacles to obtaining high performing implosions with HDC and also to develop a strategy to approach ignition conditions by starting with a relatively high adiabat and then reducing the adiabat to approach ignition relevant conditions. Implosions with low adiabat ($\alpha \sim 1.5$) pulse shapes can achieve high compression and fuel density but are more vulnerable to HI, which can adversely affect performance. High adiabat ($\alpha \sim 2$–3.5) pulse shapes achieve lower fuel densities and may not be able to reach ignition conditions; however, they provide a platform to examine implosion performance while minimizing the effects of HI. By modifying the laser pulse shape, we can then gradually reduce α and examine the trade-off between compressibility and HI.

A. Models: Hydrodynamics simulations

The HDC design was developed through a combination of 1 and 2D radiation hydrodynamics models. Most of these studies are carried out using HYDRA, which is a 3D multi-physics radiation-hydrodynamics code that attempts to include all of the physics needed to model ICF experiments.[20] Two kinds of calculations are described in this paper. 1D capsule only simulations are used to generate a suitable x-ray drive (a frequency-dependent-source or FDS: this is effectively a spectral intensity as a function of time and photon energy hν) to achieve good 1D performance. 2D integrated (hohlraum + capsule) pre-shot simulations are then used to determine the laser pulse shape required to produce this FDS source and to produce a symmetric implosion. The 2D model described here uses the "high-flux model"—electron thermal conduction with a flux-limiter f = 0.15 and the DCA non-LTE atomic physics model—developed after the NIF hohlraum energetics campaign of 2009.[21] The input laser sources are adjusted to account for backscattered light and for cross-beam transfer occurring in the hohlraum plasma.[16–18] In addition, the laser source is further degraded to match experimental shock-front and ablator data, as described by Jones *et al.*[22]

In addition, 2 and 3D capsule only simulations are used to evaluate the HI growth as a function of ablator material, ablator dopant, x-ray drive (FDS), and measured ablator roughness.[3] Dopants are added to minimize HI growth at the fuel ablator interface by reducing flux of x-rays with hυ > 1.8 keV that preheat this interface. High levels of preheat lead to a high Atwood number, increasing the risk of Rayleigh-Taylor instabilities that mix ablator and cold fuel into the hot spot.[3] Setting the dopant level is essentially a trade-off between HI at the ablation front versus at the fuel ablator interface. High levels of dopant reduce ablative and density gradient stabilization at the ablation front and so increase growth rates there. Depending on the amount of >1.8 keV x-rays, low dopant levels can allow too much preheat at the fuel ablator interface. To date, CH implosions on the NIF have used either Ge or Si dopants.[3] For HDC, the current dopant material of choice is tungsten,[23] but it is not clear what level of dopant is required. In fact, designs with no dopant are predicted to perform well for higher adiabat designs ($\alpha > 2.0$–3.5). Experiments are planned that will investigate this trade-off in detail but near term experiments with HDC have all used undoped capsules.

B. Target designs

A series of 1D and 2D simulations were carried out for HDC designs with increasing number of steps (shocks) in the x-ray drive. Table I summarizes the HDC ablator performance compared to the standard silicon doped CH (Rev 5)

This article is copyrighted as indicated in the article. Reuse of AIP content is subject to the terms at: http://scitation.aip.org/termsconditions. Downloaded to IP: 198.125.177.149 On: Wed, 04 Jun 2014 19:38:02

TABLE I. Summary of 1D performance and growth factors for HDC and CH designs.

Parameter	HDC ablator designs			CH ablator	
No. of shocks	2	3	4	4[a]	3[b]
Fuel Adiabat	3.7	2.0	1.5	1.4	2.3
Dopant	undoped	0.25% W	0.25% W	2% Si	2% Si
HI Growth factor[c]	180	2000	4000	2500	600
V_{fuel} (km/s)	380	383	380	370	380
1D yield(MJ)	0.05	17	20	17	3.2
ρR_{fuel} (g cm^{-2})	0.9	1.25	1.42	1.6	1.1

[a]Haan *et al.*[3]
[b]Dittrich *et al.*[8]
[c]Peak ablation front growth factor.[3]

$\alpha = 1.5$ (Ref. 3) and the more recent Hi-foot $\alpha \sim 2.3$ design[8] in terms of fuel adiabat, ablator dopant, HI growth factors, fuel velocity, projected 1D yield, and stagnated fuel areal density (ρR).

From Table I, it can be seen that the performance of 4-shock, $\alpha = 1.5$, HDC design is essentially equivalent to the CH 4-shock $\alpha = 1.4$ design, with slightly lower fuel ρR. The CH 3-shock Hi-foot, $\alpha \sim 2.3$, design has lower fuel density (as expected for this adiabat) and lower 1D margin than the CH 4-shock design (1D yield of 3.2 MJ vs. 17 MJ); however, it is much more stable with respect to ablation front growth (growth factor ~600 compared to 2500 for the CH 4-shock design).

The 4-shock HDC design with 0.25% atomic fraction W is even more susceptible to HI than the 4-shock CH design, as shown by the ablation front growth factors, which are 1.7× higher than the equivalent CH design. The 3-shock ($\alpha \sim 2$) HDC design (also doped with 0.25% W) has lower HI growth rates with lower compressibility, as shown by the lower fuel ρR. However, the 1D performance is comparable to the 4-shock HDC design. The laser pulse duration required to drive the 3 and 4-shock implosions is ~10 ns. This is a factor of 2.5 shorter than the equivalent CH 4-shock (22 ns) and 50% shorter than the CH 3-shock design (15 ns). A direct comparison 4-shock HDC and CH implosions can be made by comparing performance against conventional helium filled hohlraums with density around 1 mg/cc.[16–19] The helium gas reduces hohlraum wall motion, allowing a symmetric implosion to be achieved at the expense of increased backscatter and reduced hohlraum efficiency. Using the same gas filled hohlraum platform allows relatively straightforward comparison of ablator performance using a standard and well understood implosion platform, as will be described in Sec. IV.

One can also reduce the ablation front growth factors by more than a factor of 10 by using a higher adiabat ($\alpha \sim 3.7$) 2-shock pulse shape and using un-doped HDC capsules. This 2-shock pulse is not an ignition design but it is predicted to produce significant yield in 1D (50 kJ yield equivalent to ~2e16 DT neutrons), which would allow valuable insight into implosion performance while minimizing the effect of ablation front HI growth. As discussed above, the lack of dopant increases the risk of HI at the fuel-ablator interface, which can result in mixing of ablator and cold fuel into the hot spot, reducing the hot spot temperature and limiting the neutron yield. The amount of ablator mixing into the hot spot can be estimated from HDC implosions by comparing absolute x-ray and neutron yields using a 1D hotspot model[24,25] to evaluate excess impurity emission.

An even shorter laser pulse of 6 ns duration is required to generate the 2-shock x-ray drive for HDC. This short laser duration allows less time for wall motion and plasma filling and opens up the possibility of using hohlraums with very low levels of gas fill (Near Vacuum Hohlraums = NVH). The advantage with a NVH is that it has reduced backscatter, little or no hot electron generation and improved hohlraum efficiency.[26] The remaining issue with these types of hohlraums is that though reduced, plasma filling still impedes the propagation of the "inner" laser beams. These beams provide the x-ray drive to the capsule equator and impaired propagation leads to asymmetry and/ or time dependent symmetry swings through the peak of the x-ray drive. Achieving symmetry is the biggest challenge to achieving a 1D-like implosion with these hohlraums. This will be described in Sec. V. Some promising mitigation schemes using larger shape hohlraums with intermediate levels of hohlraum gas fill are described in Sec. VI.

III. EXPERIMENTAL SETUP

As shown in Fig. 2, the NIF's 192 beams are arranged into 48 quads, i.e., sets of four beams. These quads are further arranged into inner and outer cones. On each hemisphere, there are 24 quads split as follows: two overlapping inner cones consisting of 4 quads at 23.5° and 4 quads at 30° each relative to the hohlraum axis of rotation. Two sets of outer cones consist of 8 quads at 44.5° and a further 8 quads at 50° each. The inherent inner cone fraction (defined as the inner cone power divided by the total power) of the NIF is thus one third. The total laser energy and peak power delivered by each quad is measured with ±2% and ±3% accuracy, respectively.

The laser power that is backscattered out of the hohlraum is measured on one 30° inner-cone quad and one 50°

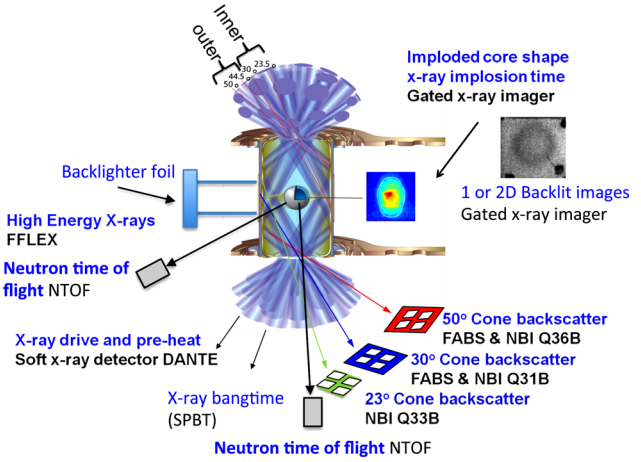

FIG. 2. Experimental setup for gold hohlraums including the equatorial x-ray self-emission, backlit images, neutron time of flight detectors, and south pole bang time detector.

This article is copyrighted as indicated in the article. Reuse of AIP content is subject to the terms at: http://scitation.aip.org/termsconditions. Downloaded to IP: 198.125.177.149 On: Wed, 04 Jun 2014 19:38:02

outer-cone with the full-aperture backscatter station (FABS) and Near Backscatter Imagers (NBI).[27] These diagnostics measure the energy, power, and spectrum of the stimulated Raman scattered (SRS), and stimulated Brillouin scattered (SBS) light that is reflected directly back towards the final optics. The SRS and SBS are measured with an error of ±20% and ±25%, respectively. The NBI measures SRS and SBS light in an f = 4 cone around the quad with an error of ± 14%. The SRS and SBS are measured with an error of ±30% for the 23.5° beam cone. For the 44.5° cone, there is no backscatter measurement and it is assumed to have the same backscatter as the 50° beam cone.

To measure the hot electrons, which can affect the ICF implosion, a filter-fluorescer array, FFLEX,[28] measures the hard x rays (>20 keV). From the hard x-ray spectrum and models of Bremsstrahlung x-ray emission due to electron scattering, the hot electron spectrum can be determined. The FFLEX has eight time integrated channels covering a range from 20 to 80 keV and two high energy time resolved channels with the energy range of 100–220 keV.

The principal x-ray drive diagnostic, Dante[29–32] is an absolutely calibrated, time-resolved 18-channel x-ray diode array that measures the x-ray flux and spectrum from 50 eV to 20 keV emitted through the laser entrance hole (LEH) at an angle of 37° to the hohlraum axis. The spectrometer uses a series of K- and L-edge filters to measure the soft x-ray flux in given bands, which can be unfolded to characterize the soft x-ray spectrum.

The principal x-ray imaging diagnostics used are x-ray framing cameras,[33] which take multiple time-resolved images of either (a) the self-emission of the imploding capsule (Symcap), (b) 1D backlit image of the imploding shell termed 1D convergent ablation (1DCONA),[34] or (c) a 2D backlit image of the imploding shell (2DCONA).[35] The 1D and 2DCONA targets have hohlraum windows on either side of the capsule and a backlighter foil chosen to give the optimum contrast to measure the shape and density of the ablator. The symcap targets only have a window on one side of the hohlraum. The x-ray framing cameras used to record self-emission or backlit images have a spatial resolution of ~10 μm and a temporal resolution of 40–80 ps. The shapes of the imploding shell and self-emission obtained from the GXD are both sensitive indicators of the symmetry of the x-ray drive. Time resolved capsule x-ray emission at 11 keV is measured by two diagnostics, first the absolutely calibrated SPBT detector looking through the lower LEH[36] and an x-ray streak camera (SPIDER) looking through the upper LEH.[37] These two instruments allow determination of the peak capsule self emission (x-ray bangtime) with an accuracy of ±50 ps. Spider measures the x-ray burn duration in 8–19 keV range with an accuracy of ±15 ps.

In order to carry out cryogenic layered implosions, the shocks must first be accurately synchronized.[10] This is achieved using a Velocity Interferometer System for an Any Reflector (VISAR) diagnostic[38,39] to measure shock timing in surrogate liquid deuterium (DD) filled "keyhole" targets, as described in detail in Robey *et al.*[40] Lastly, implosion performance is characterized using a suite of nuclear diagnostics that measure the neutron spectrum from DD and DT filled capsules (e.g., the magnetic recoil spectrometer (MRS) for DT implosions and Neutron Time of Flight (NTOF) for DD and DT implosions). These diagnostics, which have been described in detail by Frenje *et al.*,[41] measure the absolute neutron yield, ion temperature, primary and scattered neutron spectrum, neutron bang time and neutron burn duration. These observables are compared to 1 and 2D simulations of both gas filled and cryo-layered experiments to evaluate the quality of these implosions.

A. Targets: HDC and CH capsules

The experiments described here used 28 μm thick gold hohlraums, 5.75 mm in diameter, with two different lengths: 9.4 and 10.1 mm. The LEH = 3.1 mm diameter for the 9.4 mm hohlraums and 3.73 mm for the 10.1 mm hohlraums, respectively. Fig. 2 shows a schematic of the target and viewing angles of the primary diagnostics. All three target types used either a CH or HDC capsule placed in the center of the hohlraum. The hohlraums had two levels of He gas fill: (a) "conventional" gas filled hohlraums with a density of 0.96 and 1.2 mg/cc for the 4-shock CH and HDC experiments, respectively, and (b) a NVH with a density of 0.03 mg/cc for the 2-shock experiments.

For these experiments, un-doped HDC targets[42] were used with two different thicknesses; 76 μm thick for 4-shock experiments and 86 μm thick for 2-shock experiments, as shown schematically in Figures 3(a)–3(c). The performance of the 4-shock HDC implosions was compared with similar implosions using standard 4-shock pulse shapes for CH capsules in a conventional gas filled hohlraum. In this case, the CH capsule had up to 2% silicon doping and a 14 μm CH payload to match the mass of a DT ice layer[5,43] as shown in Fig. 3(d). The HDC capsules for the 2-shock experiments were ~10 μm thicker than the 4-shock in order to provide a better match for the higher drive obtained from the more efficient NVH, as described in Sec. V.

The HDC and CH targets described in this paper were filled with either pure D_2 or an equi-molar (50/50) mixtures of DT with gas density varying from 3 to 7 mg/cc. The major difference between SYMCAPs and CONA platforms is the convergent ablator experiments remove two outer quads for backlighting. In the THD 2DCONA experiment, a layer of (Tritium (75%):Hydrogen (23%):Deuterium (2%)) ice, 56 μm thick was formed on the inside of the capsule and was fielded at 1.5 K below the DT triple point. Reducing the D fraction in the fuel reduces the neutron yield produced by the implosion thus allowing high convergence cryogenic layers to be studied without large neutron background swamping x-ray diagnostics as described in detail by Glenzer *et al.*[44]

IV. GAS FILLED HOHLRAUM EXPERIMENTS (4-SHOCK PULSE SHAPE)

A four shot mini-campaign was completed using HDC capsules in 3 different target platforms. A keyhole target[40] was fielded first with a truncated laser pulse for an initial assessment of backscatter and hohlraum performance and shock timing. Two 1D convergent ablator targets were fielded to measure the in-flight capsule velocity, in-flight

This article is copyrighted as indicated in the article. Reuse of AIP content is subject to the terms at: http://scitation.aip.org/termsconditions. Downloaded to IP: 198.125.177.149 On: Wed, 04 Jun 2014 19:38:02

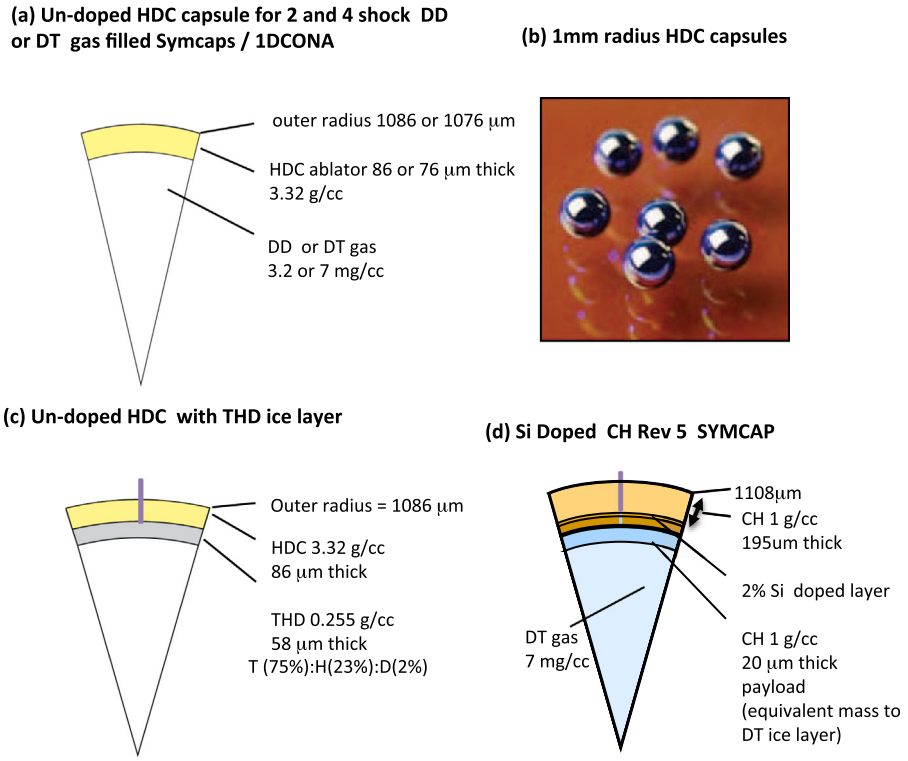

FIG. 3. Schematic pie diagrams of: (a) undoped HDC capsule with either 76 μm (4-shock experiments) or 86 μm (2-shock experiments) thick ablators, (b) picture of 1 mm radius polished HDC capsules, (c) undoped HDC ablator with THD ice layer used for the THD 2DCONA experiments, (d) silicon doped CH capsule used for CH DT filled symcap experiments.

shell thickness, and hot spot shape. The final shot in the mini-campaign was a cryogenic symcap target filled with deuterium and tritium gas to assess nuclear performance. The laser pulse shape is shown in Fig. 4 and compared with a typical CH pulse shape. A peak power of 360 TW with total laser energy of 1.3 MJ is delivered by 192 laser beams. The HDC pulse is significantly shorter than the two CH pulses due to the faster first shock transit time $\sim 1/\sqrt{}$(Picket Power $\times$ shell density).

This pulse was used to drive a 76 μm thick HDC, DT gas filled symcap. The measured laser to hohlraum coupling level of $91 \pm 2\%$ was consistent within error bars to the average of $87 \pm 3\%$ for gas filled hohlraums driving CH capsules.[11–14] The DT neutron yield of $1.6 \times 10^{15} \pm 3 \times 10^{13}$ over a nuclear burn width of 340 ps at an ion temperature of 2.9 ± 0.1 keV represents the highest gas-filled implosion yield to date. The implosion was fairly symmetric with an x-ray measured average hot spot radius, $P0 = 57 \pm 4$ μm and $P2/P0 = 0.19 \pm 0.08$, as shown in the inset of Fig. 5. Using these measured quantities and a 1D hot spot model,[25] the hot spot pressure is inferred to be 32.5 Gbar. These values are in close agreement with post-shot simulations, giving yield over simulated (1D) of 70%.

The down-scattered neutron ratio (DSR) obtained from the NTOF diagnostics was used to give further insight on the implosion conditions at stagnation. The DSR parameter is defined as the ratio of number of neutrons between 10–12 MeV and 13–15 MeV as discussed by Frenje *et al.*[41] For DT gas filled implosions, the DSR is sensitive to both the DT hot spot ρR and the remaining mass left from the ablator. For this experiment the $DSR = 0.01 \pm 0.003$, this compared well to the post shot 1D simulation of $DSR_{sim} = 0.011$ obtained from HYDRA. From these simulations, this was equivalent to an ablator $\rho R \sim 0.5$ g/cm^2. The

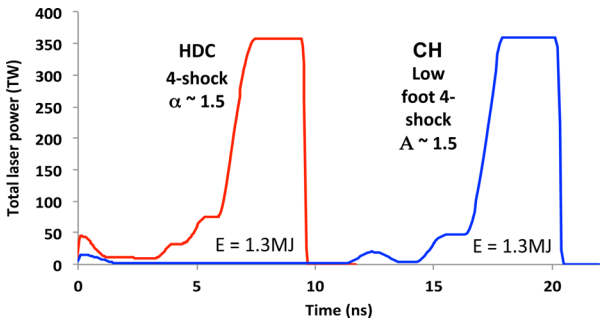

FIG. 4. The requested laser pulse shape for HDC (red line) is compared to the low-foot CH pulse (blue line). Both laser pulses have a total energy of 1.3 MJ and powers between 350 and 360 TW.

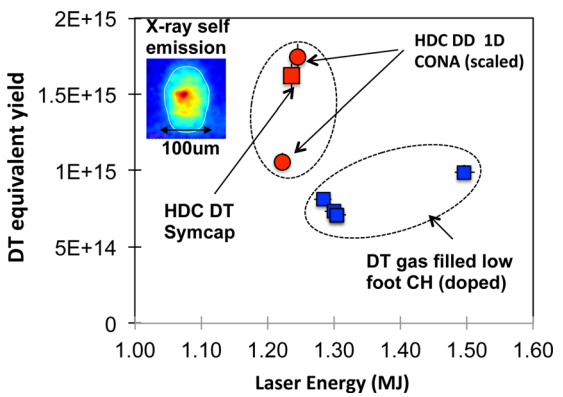

FIG. 5. DT equivalent yield vs. laser drive energy for gas filled HDC and CH 4-shock implosions driven by gas filled hohlraums. Two DD HDC implosions are included by scaling their measured DD neutron yield by a factor of 100 to account for the difference in DT vs. DD cross section at ion temperatures ~2.5–3.0 keV. Inset in top left corner shows gated x-ray image at stagnation from the HDC DT symcap.

This article is copyrighted as indicated in the article. Reuse of AIP content is subject to the terms at: http://scitation.aip.org/termsconditions. Downloaded to IP: 198.125.177.149 On: Wed, 04 Jun 2014 19:38:02

inflight ablator thickness was also measured to be 45 μm at R = 300 μm from the 1DCONA experiments. This was also in good agreement with the 1D simulations and consistent with the near 1D performance of these gas filled HDC implosions.

The performance of this symcap compared to an equivalent CH gas filled implosions is also shown in Fig. 5, where the measured DT (or DD yield scaled by factor of 100) yield plotted as a function of laser drive energy. The HDC experiment produced a yield 2× higher than any previous CH gas-filled symcaps, which have a similar convergence ratio.

Although this is a very encouraging result, it must be noted that in order to match the 2D simulations drive must be significantly degraded using drive multipliers following the same methodology of Jones.[22] These drive multipliers are very similar to those applied to gas-filled hohlraums driving 4-shock CH capsules, representing an unexplained ~25% loss in peak drive compared to simulations. In addition, although the laser coupling was high at 91 ± 2%, this still represents significant backscatter. Combining these factors represents an energy loss of ~200 kJ, which appears to remain a fundamental issue related to the energetics of gas filled hohlraums.[16–19] One possible solution to this issue is to use 2-shock pulses with HDC ablators in near vacuum hohlraums, which have demonstrated low levels of backscatter and high coupling.[26]

V. NEAR VACUUM HOHLRAUMS (2-SHOCK PULSE SHAPE)

As discussed in Sec. II, the short laser duration of the 2-shock HDC pulse (as shown in Fig. 6) allows the possibility that a low gas filled hohlraum can be used to achieve a symmetric implosion with low backscatter and good efficiency. A mini campaign of three shots was used to investigate the performance. A keyhole target was again fielded first with a truncated laser pulse for an initial assessment of backscatter and hohlraum performance and shock timing. A gas filled cryogenic symcap target filled with deuterium gas was used to assess symmetry and nuclear performance. Finally, the implosion velocity and inflight ablator shape

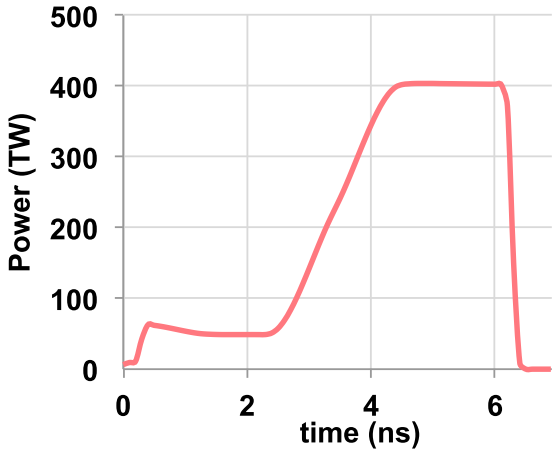

FIG. 6. 2-shock laser pulse shape for driving a symcap in a near vacuum hohlraum with 86 μm thick undoped HDC ablator. The laser energy was 1.3 MJ with peak power of 400 TW.

pushing a THD ice layer was measured using a 2D THDCONA experiment.

Standard 5.75 mm diameter hohlraum targets were used for these experiments (as described in Sec. III), but with a minimal helium gas fill of 0.032 mg/cc, required to provide conduction cooling of the capsule. Unlike conventional gas-filled hohlraums, in a NVH there is no transfer of energy between the inner and outer beams at peak power and so the implosion symmetry is set by direct adjustments to cone energies. The lack of hohlraum gas also leads to minimal backscatter losses and very efficient drive as shown in the performance of an 86 μm thick un-doped HDC capsule filled with 3 mg/cc DD gas. Table II summarizes the NVH implosion experiment as compared to post-shot 1D modeling. As expected, the laser to hohlraum coupling was 98% and the implosion (at 10× convergence) achieved a record neutron yield of 2.4e13 for a DD gas-filled implosion. The implosion was symmetric and was well described by post-shot simulations when the simulated M band (x-rays > 1.8 keV) was adjusted to match the experimentally measured value. The x-ray bang-time of 7.8 ns was consistent with an extremely high inferred shell velocity of 430 km/s.

The excellent performance of the symcap implosion is very promising for HDC but cryogenic ice layers with convergence >20× are a more challenging test of implosion performance. A convergent ablation measurement on a THD ice layer provides information on both the implosion velocity and inflight shell shape close to bang time. In addition, measurements of the nuclear performance and absolute x-ray emission allow an estimate of ablator mix into the hot spot.[24,25]

A truncated version of the 2-shock pulse shape, with laser energy 1.25 MJ, was used to drive an 86 μm thick HDC ablator with a 56 μm thick THD ice layer (T(75%):H(23%):D(2%)). The implosion was characterized using 2D backlighting with a 7.8 keV nickel He−α backlighter onto a gated x-ray detector, as described in Sec. II. The THD 2DCONA target is shown in Fig. 7. The nickel backlighter was driven by 8 beams of NIF and timed to observe the shell shape 350–100ps before bang time. Data from this experiment are shown in Fig. 8. Strong capsule self-emission and low contrast images meant that only the first 4 frames in "strip 1" could be analyzed for shape and velocity. The shell was quite round with P2 = 2 μm at a capsule radius

TABLE II. Comparison of post-shot calculated vs measured implosion performance for a DD filled HDC target driven by a NVH with a 2-shock pulse shape.

Parameter	Experiment (N130813)	1D Post shot simulation[a]
M band fraction (x-rays > 1.8 keV)	22%	22%
Yield (DD)	2.3e13	2.4e13
Tion (keV)	3.4	3.3
Laser–Hohl coupling	98%	N/A
Bangtime	7.77	7.75
Radius (P0) (μm)	91	101
Velocity (km/s)	N/A	430

[a]Drive adjusted for delivered energy and observed spectrum.

This article is copyrighted as indicated in the article. Reuse of AIP content is subject to the terms at: http://scitation.aip.org/termsconditions. Downloaded to IP: 198.125.177.149 On: Wed, 04 Jun 2014 19:38:02

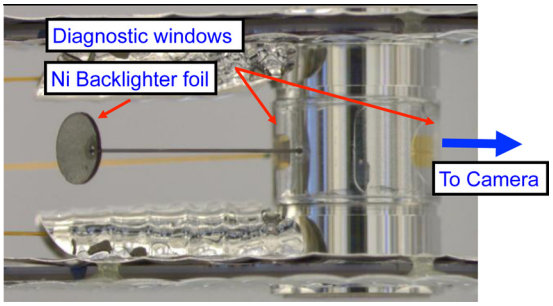

FIG. 7. 2DCONA target showing hohlraum with Ni back lighter foil and diagnostic windows.

P0 = 200 μm when the shell velocity reached 385 ± 20 km/s. This is consistent with an inferred fuel velocity 410 ± 20 km/s, obtained by comparison with HYDRA post shot simulations (see Meezan *et al.*[5] for methodology to extract inferred fuel velocities from CONA shell velocity measurements). The inferred fuel velocity vs ablator remaining mass is shown in Fig. 9 for this HDC implosion compared to CH THD layered implosion in a gas-filled hohlraum driven by a 1.6 MJ 4-shock laser pulse. HYDRA post shot simulations for these two implosions are also shown. These data and simulations illustrate the increased drive of a NVH, which achieves significantly higher velocity and more ablated mass for less laser energy than gas filled hohlraum implosions using a CH ablator.

An estimate of the ablator mixing into the hot spot was obtained from measurements of the neutron yield, ion temperature, and absolute x-ray emission at 11 keV measured by the SPBT detector.[36] By comparing the observed x-ray emissivity with that expected from a pure DT plasma, one can infer the amount of high Z (carbon) in the hotspot.[24,25] Results for the THD experiment are shown in Fig. 10 compared to a series of CH DT layered implosions. The HDC THD implosion was consistent with zero inferred hotspot mix (<90 ng). This is a very promising result, confirming

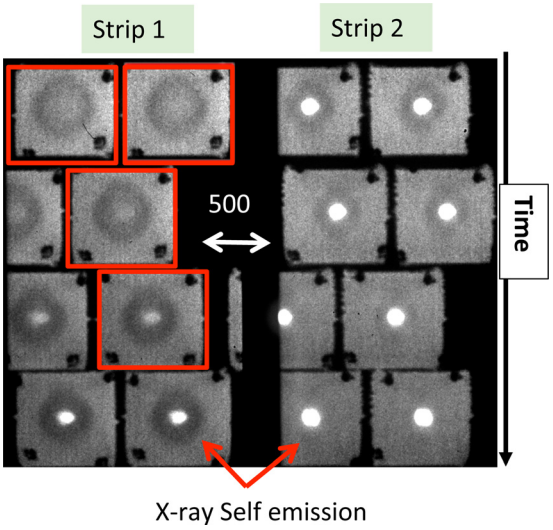

FIG. 8. 2D radiography data using 7.8 keV x-rays backlighting the imploding HDC capsule from 350ps before up to peak x-ray emission (bang time). The 4 frames used in the velocity analysis are outlined in red.

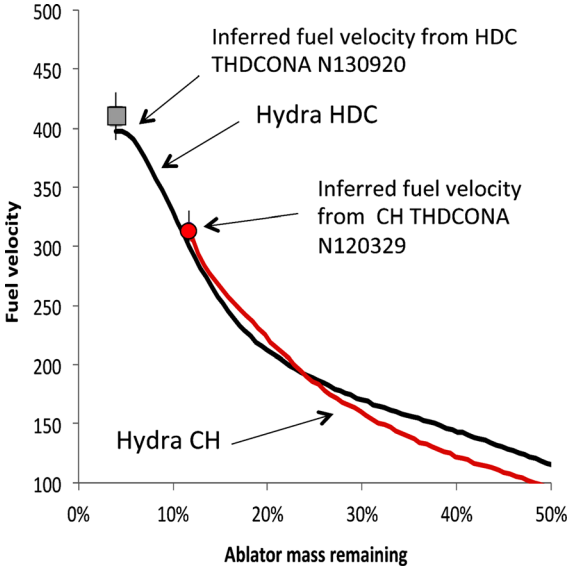

FIG. 9. Inferred fuel velocity vs. Ablator mass remaining for HDC NVH and equivalent CH implosion experiment from a gas filled hohlraum. Also shown are HYDRA post-shot simulations for these implosions.

low hot spot mix in a high velocity implosion, consistent with low ablation front growth rates and pre-shot simulations that predicted low fuel ablator mix for the x-ray drive and level of M band measured in the experiment.

There is however an issue with hot spot symmetry that prevents this implosion from being truly 1D. Pre and post shot 2D simulations indicated that the inner laser beam propagation is impaired late in the drive (around 6 ns) by hohlraum wall motion and plasma filling. In these experiments, this was partially overcome by using dynamic beam phasing between the inner and outer cones. Specifically, the inner cone fraction was set high early on the rise to peak power. This allowed drive to reach the equator when a channel was still open, but at the expense of driving a P2 symmetry swing, which in turn generated hydrodynamic jets from the polar regions. This reduced the yield to 10%–20% of the 1D value, much lower than the lower convergence symcap. Some improvements can be made by repointing the beams

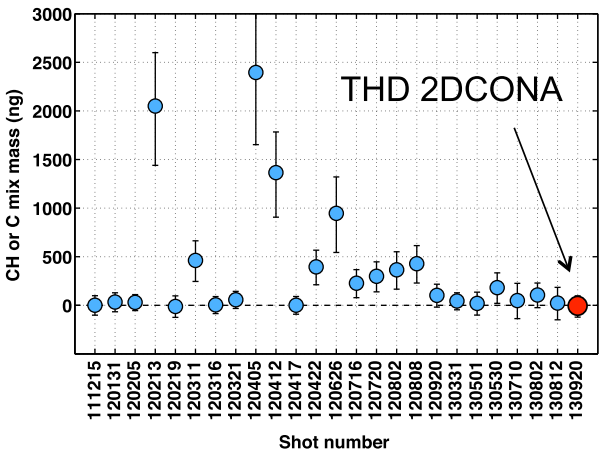

FIG. 10. Plot of inferred ng of CH or C mass mixed into the hotspot as a function of shot number for a series of CH implosions and the THD 2DCONA using the HDC ablator.

This article is copyrighted as indicated in the article. Reuse of AIP content is subject to the terms at: http://scitation.aip.org/termsconditions. Downloaded to IP: 198.125.177.149 On: Wed, 04 Jun 2014 19:38:02

but true 1D implosions may require more radical changes to the hohlraum size and shape.

VI. CONCLUSIONS AND DISCUSSION

HDC ablators have been shown to perform well in ICF implosions using both conventional gas filled and near vacuum hohlraums. Performance in gas filled hohlraums was essentially limited by the hohlraum energetics. HDC produced higher quality implosions than equivalent CH designs. Near vacuum hohlraums have provided an alternate path for higher adiabat implosions with very high velocities and little or no hotspot mix. These high velocities, in excess of the 400 km/s required for ignition designs, indicate that the hohlraum size can be increased for fixed capsule radius while maintaining adequate drive to achieve ignition velocities. Increasing the case to capsule ratio in this way creates more room for inner beam propagation potentially reducing the need for dynamic beam phasing. Similarly, reshaping the hohlraum near the laser entrance holes can reduce hohlraum wall plasma blow off in the path of the inner beams, improving the drive to the capsule equator. Finally, choosing an intermediate hohlraum gas density should also reduce hohlraum wall plasma filling, further improving inner beam propagation while keeping below thresholds for laser plasma instabilities. A series of 2D simulations indicate that by using all three of these tools, time dependent symmetry should be improved for pulses as long as 9 ns. If this can be realized, this opens up the possibility of extending the promising near vacuum hohlraums to lower adiabat pulses (such as the 10 ns duration 3-shock pulses, $\alpha \sim 2$). A series of experiments are planned to examine this parameter space.

ACKNOWLEDGMENTS

The authors acknowledge the efforts of the NIF operations, laser performance, target diagnostics, and target fabrication teams. This work was performed under the auspices of the U.S. Department of Energy by Lawrence Livermore National Laboratory under Contract No. DE-AC52-07NA27344.

[1]J. Lindl, P. Amendt, R. Berger, S. Glendinning, S. Glenzer, S. Haan, R. Kauffman, O. Landen, and L. Suter, Phys. Plasmas **11**, 339 (2004).
[2]E. Moses, R. Boyd, B. Remington, C. Keane, and R. Al-Ayat, Phys. Plasmas **16**, 041006 (2009).
[3]S. W. Haan, J. D. Lindl, D. A. Callahan, D. S. Clark, J. D. Salmonson, B. A. Hammel, L. J. Atherton, R. C. Cook, M. J. Edwards, S. Glenzer, A. V. Hamza, S. P. Hatchett, M. C. Herrmann, D. E. Hinkel, D. D. Ho, H. Huang, O. S. Jones, J. Kline, G. Kyrala, O. L. Landen, B. J. MacGowan, M. M. Marinak, D. D. Meyerhofer, J. L. Milovich, K. A. Moreno, E. I. Moses, D. H. Munro, A. Nikroo, R. E. Olson, K. Peterson, S. M. Pollaine, J. E. Ralph, H. F. Robey, B. K. Spears, P. T. Springer, L. J. Suter, C. A. Thomas, R. P. Town, R. Vesey, S. V. Weber, H. L. Wilkens, and D. C. Wilson, Phys. Plasmas **18**, 051001 (2011).
[4]Y. Saillard, Nucl. Fusion **46**, 1017 (2006).
[5]N. B. Meezan, A. J. MacKinnon, D. G. Hicks, E. L. Dewald, R. Tommasini, S. Le Pape, T. Doppner, T. Ma, D. R. Farley, D. H. Kalantar, P. Di Nicola, D. A. Callahan, H. F. Robey, C. A. Thomas, S. T. Prisbrey, O. S. Jones, J. L. Milovich, D. S. Clark, D. C. Eder, M. B. Schneider, K. Widmann, J. A. Koch, J. D. Salmonson, Y. P. Opachich, L. R. Benedetti, S. F. Khan, A. G. MacPhee, S. M. Glenn, D. K. Bradley, E. G. Dzenitis, B. R. Nathan, J. J. Kroll, A. V. Hamza, S. N. Dixit, L. J. Atherton, O. L. Landen, S. H. Glenzer, W. W. Hsing, L. J. Suter, M. J. Edwards, B. J. MacGowan, and E. I. Moses, Phys. Plasmas **20**, 056311 (2013).
[6]M. J. Edwards, P. K. Patel, J. D. Lindl, L. J. Atherton, S. H. Glenzer, S. W. Haan, J. D. Kilkenny, O. L. Landen, E. I. Moses, A. Nikroo, R. Petrasso, T. C. Sangster, P. T. Springer, S. Batha, R. Benedetti, L. Bernstein, R. Betti, D. L. Bleuel, T. R. Boehly, D. K. Bradley, J. A. Caggiano, D. A. Callahan, P. M. Celliers, C. J. Cerjan, K. C. Chen, D. S. Clark, G. W. Collins, E. L. Dewald, L. Divol, S. Dixit, T. Doeppner, D. H. Edgell, J. E. Fair, M. Farrell, R. J. Fortner, J. Frenje, M. G. Gatu Johnson, E. Giraldez, V. Yu. Glebov, G. Grim, B. A. Hammel, A. V. Hamza, D. R. Harding, S. P. Hatchett, N. Hein, H. W. Herrmann, D. Hicks, D. E. Hinkel, M. Hoppe, W. W. Hsing, N. Izumi, B. Jacoby, O. S. Jones, D. Kalantar, R. Kauffman, J. L. Kline, J. P. Knauer, J. A. Koch, B. J. Kozioziemski, G. Kyrala, K. N. LaFortune, S. Le Pape, R. J. Leeper, R. Lerche, T. Ma, B. J. MacGowan, A. J. MacKinnon, A. Macphee, E. R. Mapoles, M. M. Marinak, M. Mauldin, P. W. McKenty, M. Meezan, P. A. Michel, J. Milovich, J. D. Moody, M. Moran, D. H. Munro, C. L. Olson, K. Opachich, A. E. Pak, T. Parham, H.-S. Park, J. E. Ralph, S. P. Regan, B. Remington, H. Rinderknecht, H. F. Robey, M. Rosen, S. Ross, J. D. Salmonson, J. Sater, D. H. Schneider, F. H. Séguin, S. M. Sepke, D. A. Shaughnessy, V. A. Smalyuk, B. K. Spears, C. Stoeckl, W. Stoeffl, L. Suter, C. A. Thomas, R. Tommasini, R. P. Town, S. V. Weber, P. J. Wegner, K. Widman, M. Wilke, D. C. Wilson, C. B. Yeamans, and A. Zylstra, Phys. Plasmas **20**, 070501 (2013).
[7]A. J. Mackinnon, J. L. Kline, S. N. Dixit, S. H. Glenzer, M. J. Edwards, D. A. Callahan, N. B. Meezan, S. W. Haan, J. D. Kilkenny, T. Döppner, D. R. Farley, J. D. Moody, J. E. Ralph, B. J. MacGowan, O. L. Landen, H. F. Robey, T. R. Boehly, P. M. Celliers, J. H. Eggert, K. Krauter, G. Frieders, G. F. Ross, D. G. Hicks, R. E. Olson, S. V. Weber, B. K. Spears, J. D. Salmonsen, P. Michel, L. Divol, B. Hammel, C. A. Thomas, D. S. Clark, O. S. Jones, P. T. Springer, C. J. Cerjan, G. W. Collins, V. Y. Glebov, J. P. Knauer, C. Sangster, C. Stoeckl, P. McKenty, J. M. McNaney, R. J. Leeper, C. L. Ruiz, G. W. Cooper, A. G. Nelson, G. G. A. Chandler, K. D. Hahn, M. J. Moran, M. B. Schneider, N. E. Palmer, R. M. Bionta, E. P. Hartouni, S. LePape, P. K. Patel, N. Izumi, R. Tommasini, E. J. Bond, J. A. Caggiano, R. Hatarik, G. P. Grim, F. E. Merrill, D. N. Fittinghoff, N. Guler, O. Drury, D. C. Wilson, H. W. Herrmann, W. Stoeffl, D. T. Casey, M. G. Johnson, J. A. Frenje, R. D. Petrasso, A. Zylestra, H. Rinderknecht, D. H. Kalantar, J. M. Dzenitis, P. Di Nicola, D. C. Eder, W. H. Courdin, G. Gururangan, S. C. Burkhart, S. Friedrich, D. L. Blueuel, L. A. Bernstein, M. J. Eckart, D. H. Munro, S. P. Hatchett, A. G. Macphee, D. H. Edgell, D. K. Bradley, P. M. Bell, S. M. Glenn, N. Simanovskaia, M. A. Barrios, R. Benedetti, G. A. Kyrala, R. P. J. Town, E. L. Dewald, J. L. Milovich, K. Widmann, A. S. Moore, G. LaCaille, S. P. Regan, L. J. Suter, B. Felker, R. C. Ashabranner, M. C. Jackson, R. Prasad, M. J. Richardson, T. R. Kohut, P. S. Datte, G. W. Krauter, J. J. Klingman, R. F. Burr, T. A. Land, M. R. Hermann, D. A. Latray, R. L. Saunders, S. Weaver, S. J. Cohen, L. Berzins, S. G. Brass, E. S. Palma, R. R. Lowe-Webb, G. N. McHalle, P. A. Arnold, L. J. Lagin, C. D. Marshall, G. K. Brunton, D. G. Mathisen, R. D. Wood, J. R. Cox, R. B. Ehrlich, K. M. Knittel, M. W. Bowers, R. A. Zacharias, B. K. Young, J. P. Holder, J. R. Kimbrough, T. Ma, K. N. La Fortune, C. C. Widmayer, M. J. Shaw, G. V. Erbert, K. S. Jancaitis, J. M. DiNicola, C. Orth, G. Heestand, R. Kirkwood, C. Haynam, P. J. Wegner, P. K. Whitman, A. Hamza, E. G. Dzenitis, R. J. Wallace, S. D. Bhandarkar, T. G. Parham, R. Dylla-Spears, E. R. Mapoles, B. J. Kozioziemski, J. D. Sater, C. F. Walters, B. J. Haid, J. Fair, A. Nikroo, E. Giraldez, K. Moreno, B. Vanwonterghem, R. L. Kauffman, S. Batha, D. W. Larson, R. J. Fortner, D. H. Schneider, J. D. Lindl, R. W. Patterson, L. J. Atherton, and E. I. Moses, Phys. Rev. Lett. **108**, 215005 (2012); V. A. Smalyuk, L. J. Atherton, L. R. Benedetti, R. Bionta, D. Bleuel, E. Bond, D. K. Bradley, J. Caggiano, D. A. Callahan, D. T. Casey, P. M. Celliers, C. J. Cerjan, D. Clark, E. L. Dewald, S. N. Dixit, T. Döppner, D. H. Edgell, M. J. Edwards, J. Frenje, M. Gatu-Johnson, V. Y. Glebov, S. Glenn, S. H. Glenzer, G. Grim, S. W. Haan, B. A. Hammel, E. P. Hartouni, R. Hatarik, S. Hatchett, D. G. Hicks, W. W. Hsing, N. Izumi, O. S. Jones, M. H. Key, S. F. Khan, J. D. Kilkenny, J. L. Kline, J. Knauer, G. A. Kyrala, O. L. Landen, S. Le Pape, J. D. Lindl, T. Ma, B. J. MacGowan, A. J. Mackinnon, A. G. MacPhee, J. McNaney, N. B. Meezan, J. D. Moody, A. Moore, M. Moran, E. I. Moses, A. Pak, T. Parham, H.-S. Park, P. K. Patel, R. Petrasso, J. E. Ralph, S. P. Regan, B. A. Remington, H. F. Robey, J. S. Ross, B. K. Spears, P. T. Springer, L. J. Suter, R. Tommasini, R. P. Town, S. V. Weber, and K. Widmann, *ibid.* **111**, 215001 (2013).
[8]T. R. Dittrich, O. A. Hurricane, D. A. Callahan, E. L. Dewald, T. Döppner, D. E. Hinkel, L. F. Berzak Hopkins, S. Le Pape, T. Ma, J. L. Milovich,

This article is copyrighted as indicated in the article. Reuse of AIP content is subject to the terms at: http://scitation.aip.org/termsconditions. Downloaded to IP: 198.125.177.149 On: Wed, 04 Jun 2014 19:38:02

J. C. Moreno, P. K. Patel, H.-S. Park, B. A. Remington, J. D. Salmonson, and J. L. Kline, Phys. Rev. Lett. **112**, 055002 (2014).
[9]H.-S. Park, O. A. Hurricane, D. A. Callahan, D. T. Casey, E. L. Dewald, T. R. Dittrich, T. Döppner, D. E. Hinkel, L. F. Berzak Hopkins, S. Le Pape, T. Ma, P. K. Patel, B. A. Remington, H. F. Robey, J. D. Salmonson, and J. L. Kline, Phys. Rev. Lett. **112**, 055001 (2014).
[10]O. L. Landen, J. Edwards, S. W. Haan, H. F. Robey, J. Milovich, B. K. Spears, S. V. Weber, D. S. Clark, J. D. Lindl, B. J. MacGowan, E. I. Moses, J. Atherton, P. A. Amendt, T. R. Boehly, D. K. Bradley, D. G. Braun, D. A. Callahan, P. M. Celliers, G. W. Collins, E. L. Dewald, L. Divol, J. A. Frenje, S. H. Glenzer, A. Hamza, B. A. Hammel, D. G. Hicks, N. Hoffman, N. Izumi, O. S. Jones, J. D. Kilkenny, R. K. Kirkwood, J. L. Kline, G. A. Kyrala, M. M. Marinak, N. Meezan, D. D. Meyerhofer, P. Michel, D. H. Munro, R. E. Olson, A. Nikroo, S. P. Regan, L. J. Suter, C. A. Thomas, and D. C. Wilson, Phys. Plasmas **18**, 051002 (2011).
[11]D. G. Hicks, T. R. Boehly, P. M. Celliers, D. K. Bradley, J. H. Eggert, R. S. McWilliams, R. Jeanloz, and G. W. Collins, Phys. Rev. B **78**, 174102 (2008).
[12]M. D. Knudson, M. P. Desjarlais, and D. H. Dolan, Science **322**, 1822 (2008).
[13]P. M. Celliers, D. J. Erskine, C. M. Sorce, D. G. Braun, O. L. Landen, and G. W. Collins, Rev. Sci. Instrum. **81**, 035101 (2010).
[14]O. L. Landen, D. K. Bradley, D. G. Braun, V. A. Smalyuk, D. G. Hicks, P. M. Celliers, S. Prisbrey, R. Page, T. R. Boehly, S. W. Haan, D. H. Munro, R. G. Wallace, A. Nikroo, A. Hamza, J. Biener, C. Wild, E. Woerner, R. E. Olson, G. A. Rochau, M. Knudson, D. C. Wilson, H. F. Robey, G. W. Collins, D. Ho, J. Edwards, M. M. Marinak, B. A. Hammel, D. D. Meyerhofer, and B. J. MacGowan, J. Phys.: Conf. Ser. **112**, 022004 (2008).
[15]T. R. Boehly, D. L. Brown, R. S. Craxton, R. L. Keck, J. P. Knauer, J. H. Kelly, T. J. Kessler, S. A. Kumpan, S. J. Loucks, S. A. Letzring, F. J. Marshall, R. L. McCrory, S. F. B. Morse, W. Seka, J. M. Soures, and C. P. Verdon, Opt. Commun. **133**, 495 (1997).
[16]R. P. J. Town, M. D. Rosen, P. A. Michel, L. Divol, J. D. Moody, G. A. Kyrala, M. B. Schneider, J. L. Kline, C. A. Thomas, J. L. Milovich, D. A. Callahan, N. B. Meezan, D. E. Hinkel, E. A. Williams, R. L. Berger, M. J. Edwards, L. J. Suter, S. W. Haan, J. D. Lindl, E. L. Dewald, S. Dixit, S. H. Glenzer, O. L. Landen, E. I. Moses, H. A. Scott, J. A. Harte, and G. B. Zimmerman, Phys. Plasmas **18**, 056302 (2011).
[17]P. Michel, L. Divol, E. Williams, S. Weber, C. Thomas, D. Callahan, S. Haan, J. Salmonson, S. Dixit, D. Hinkel, M. Edwards, B. MacGowan, J. Lindl, S. Glenzer, and L. Suter, Phys. Rev. Lett. **102**, 025004 (2009).
[18]P. Michel, S. H. Glenzer, L. Divol, D. K. Bradley, D. Callahan, S. Dixit, S. Glenn, D. Hinkel, R. K. Kirkwood, J. L. Kline, W. L. Kruer, G. A. Kyrala, S. L. Pape, N. B. Meezan, R. Town, K. Widmann, E. A. Williams, B. J. MacGowan, J. Lindl, and L. J. Suter, Phys. Plasmas **17**, 056305 (2010).
[19]J. D. Moody, D. H. Callahan, D. Hinkel, P. A. Amendt, K. L. Baker, D. Bradley, P. M. Celliers, E. L. Dewald, L. Divol, T. Döppner, D. C. Eder, M. J. Edwards, O. Jones, S. W. Haan, D. Ho, L. B. Hopkins, N. Izumi, D. Kalantar, R. L. Kauffman, J. D. Kilkenny, O. Landen, B. Lasinski, S. LePape, T. Ma, B. J. MacGowan, S. A. MacLaren, A. J. Mackinnon, D. Meeker, N. Meezan, P. Michel, J. L. Milovich, D. Munro, A. E. Pak, M. Rosen, J. Ralph, H. F. Robey, J. S. Ross, D. Strozzi, E. Storm, C. Thomas, R. P. J. Town, K. L. Widmann, J. Kline, G. Kyrala, A. Nikroo, T. Boehly, A. S. Moore, and S. H. Glenzer, Phys. Plasmas **21**, 056317 (2014).
[20]M. M. Marinak, G. D. Kerbel, N. A. Gentile, O. Jones, D. Munro, S. Pollaine, T. R. Dittrich, and S. W. Haan, Phys. Plasmas **8**, 2275 (2001).
[21]M. Rosen, H. Scott, D. Hinkel, E. Williams, D. Callahan, R. Town, L. Divol, P. Michel, W. Kruer, L. Suter, R. London, J. Harte, and G. Zimmerman, High Energy Density Phys. **7**, 180 (2011).
[22]O. S. Jones, C. J. Cerjan, M. M. Marinak, J. L. Milovich, H. F. Robey, P. T. Springer, L. R. Benedetti, D. L. Bleuel, E. J. Bond, D. K. Bradley, D. A. Callahan, J. A. Caggiano, P. M. Celliers, D. S. Clark, S. M. Dixit, T. Doppner, R. J. Dylla-Spears, E. G. Dzentitis, D. R. Farley, S. M. Glenn, S. H. Glenzer, S. W. Haan, B. J. Haid, C. A. Haynam, D. G. Hicks, B. J. Kozioziemski, K. N. LaFortune, O. L. Landen, E. R. Mapoles, A. J. MacKinnon, J. M. McNaney, N. B. Meezan, P. A. Michel, J. D. Moody, M. J. Moran, D. H. Munro, M. V. Patel, T. G. Parham, J. D. Sater, S. M. Sepke, B. K. Spears, R. P. J. Town, S. V. Weber, K. Widmann, C. C. Widmayer, E. A. Williams, L. J. Atherton, M. J. Edwards, J. D. Lindl, B. J. MacGowan, L. J. Suter, R. E. Olson, H. W. Herrmann, J. L. Kline, G. A. Kyrala, D. C. Wilson, J. Frenje, T. R. Boehly, V. Glebov, J. P. Knauer, A. Nikroo, H. Wilkens, and J. D. Kilkenny, Phys. Plasmas **19**, 056315 (2012).
[23]M. M. Biener, J. Biener, S. O. Kucheyev, Y. M. Wang, B. El-Dasher, N. E. Teslich, A. V. Hamza, H. Obloh, W. Mueller-Sebert, M. Wolfer, T. Fuchs, M. Grimm, A. Kriele, and C. Wild, Diamond Relat. Mater. **19**, 643–647 (2010).
[24]T. Ma, P. K. Patel, N. Izumi, P. T. Springer, M. H. Key, L. J. Atherton, L. R. Benedetti, D. K. Bradley, D. A. Callahan, P. M. Celliers, C. J. Cerjan, D. S. Clark, E. L. Dewald, S. N. Dixit, T. Döppner, D. H. Edgell, R. Epstein, S. Glenn, G. Grim, S. W. Haan, B. A. Hammel, D. Hicks, W. W. Hsing, O. S. Jones, S. F. Khan, J. D. Kilkenny, J. L. Kline, G. A. Kyrala, O. L. Landen, S. Le Pape, B. J. MacGowan, A. J. Mackinnon, A. G. MacPhee, N. B. Meezan, J. D. Moody, A. Pak, T. Parham, H.-S. Park, J. E. Ralph, S. P. Regan, B. A. Remington, H. F. Robey, J. S. Ross, B. K. Spears, V. Smalyuk, L. J. Suter, R. Tommasini, R. P. Town, S. V. Weber, J. D. Lindl, M. J. Edwards, S. H. Glenzer, and E. I. Moses, Phys. Rev. Lett. **111**, 085004 (2013).
[25]C. Cerjan, P. Springer, and S. Sepke, Phys. Plasmas **20**, 056319 (2013).
[26]R. E. Olson, L. J. Suter, J. L. Kline, D. A. Callahan, M. D. Rosen, S. N. Dixit, O. L. Landen, N. B. Meezan, J. D. Moody, C. A. Thomas, A. Warrick, K. Widmann, E. A. Williams, and S. H. Glenzer, Phys. Plasmas **19**, 053301 (2012); S. Le Pape, L. Divol, L. Berzak Hopkins, A. Mackinnon, N. Meezan, D. Casey, J. Frenje, H. Herrmann, J. McNaney, T. Ma, K. Widmann, A. Pak, G. Grimm, J. Knauer, R. Petrasso, A. Zylstra, H. Rinderknecht, and J. D. Kilkenny, "Observation of a reflected shock in an indirectly-driven spherical implosion on the National Ignition Facility," Phys. Rev. Lett. (to be published).
[27]J. D. Moody, P. Datte, K. Krauter, E. Bond, P. A. Michel, S. H. Glenzer, L. Divol, C. Niemann, L. Suter, N. Meezan, B. J. MacGowan, R. Hibbard, R. London, J. Kilkenny, R. Wallace, J. L. Kline, K. Knittel, G. Frieders, B. Golick, G. Ross, K. Widmann, J. Jackson, S. Vernon, and T. Clancy, Rev. Sci. Instrum. **81**, 10D921 (2010).
[28]E. L. Dewald, C. Thomas, S. Hunter, L. Divol, N. Meezan, S. H. Glenzer, L. J. Suter, E. Bond, J. L. Kline, J. Celeste, D. Bradley, P. Bell, R. L. Kauffman, J. Kilkenny, and O. L. Landen, Rev. Sci. Instrum. **81**, 0D938 (2010).
[29]R. L. Kauffman, H. N. Kornblum, D. W. Phillion, C. B. Darrow, B. F. Lasinski, L. J. Suter, A. R. Theissen, R. J. Wallace, and F. Ze, Rev. Sci. Instrum. **66**, 678 (1995).
[30]H. N. Kornblum, R. L. Kauffman, and J. A. Smith, Rev. Sci. Instrum. **57**, 2179 (1986).
[31]E. L. Dewald, K. M. Campbell, R. E. Turner, J. P. Holder, O. L. Landen, S. H. Glenzer, R. L. Kauffman, L. J. Suter, M. Landon, M. Rhodes, and D. Lee, Rev. Sci. Instrum. **75**, 3579 (2004).
[32]J. L. Kline, K. Widmann, A. Warrick, R. E. Olson, C. A. Thomas, A. S. Moore, L. J. Suter, O. Landen, D. Callahan, S. Azevedo, J. Liebman, S. H. Glenzer, A. Conder, S. N. Dixit, P. Torres III, V. Tran, E. L. Dewald, J. Kamperschroer, L. J. Atherton, R. Beeler, Jr., L. Berzins, J. Celeste, C. Haynam, W. Hsing, D. Larson, B. J. MacGowan, D. Hinkel, D. Kalantar, R. Kauffman, J. Kilkenny, N. Meezan, M. D. Rosen, M. Schneider, E. A. Williams, S. Vernon, R. J. Wallace, B. Van Wonterghem, and B. K. Young, Rev. Sci. Instrum. **81**, 10E321 (2010).
[33]G. A. Kyrala, S. Dixit, S. Glenzer, D. Kalantar, D. Bradley, N. Meezan Izumi, N. O. L. Landen, D. Callahan, S. V. Weber, J. P. Holder, S. Glenn, M. J. Edwards, P. Bell, J. Kimbrough, J. Koch, R. Prasad, L. Suter, J. L. Kline, and J. Kilkenny, Rev. Sci. Instrum. **81**, 10E316 (2010).
[34]D. G. Hicks, N. B. Meezan, E. L. Dewald, A. J. Mackinnon, D. A. Callahan, T. Doeppner, L. R. Benedetti, D. K. Bradley, P. M. Celliers, D. S. Clark, S. N. Dixit, E. G. Dzenitis, J. E. Eggert, D. R. Farley, S. M. Glenn, S. H. Glenzer, A. V. Hamza, R. F. Heeter, J. P. Holder, N. Izumi, D. H. Kalantar, S. F. Khan, J. J. Kroll, T. Ma, A. G. MacPhee, J. M. McNaney, J. D. Moody, M. J. Moran, B. R. Nathan, K. P. Opachich, R. R. Prasad, J. E. Ralph, H. F. Robey, J. R. Rygg, J. D. Salmonson, M. B. Schneider, N. Simanovskaia, B. K. Spears, R. Tommasini, K. Widmann, G. W. Collins, O. L. Landen, J. D. Kilkenny, W. W. Hsing, B. J. MacGowan, L. J. Atherton, M. J. Edwards, R. E. Olson, J. A. Frenje, R. D. Petrasso, H. G. Rinderknecht, A. B. Zylstra, J. L. Kline, G. A. Kyrala, and A. Nikroo, Phys. Plasmas **19**, 122702 (2012).
[35]J. R. Rygg, O. S. Jones, J. E. Field, M. A. Barrios, L. R. Benedetti, G. W. Collins, D. C. Eder, M. J. Edwards, J. L. Kline, J. J. Kroll, O. L. Landen, T. Ma, A. Pak, J. L. Peterson, K. Raman, R. P. J. Town, and D. K. Bradley, Phys. Rev. Lett. (to be published).
[36]D. H. Edgell, D. K. Bradley, E. J. Bond, S. Burns, D. A. Callahan, J. Celeste, M. J. Eckart, V. Yu. Glebov, D. S. Hey, G. Lacaille, J. D. Kilkenny, J. Kimbrough, A. J. Mackinnon, J. Magoon, J. Parker, T. C. Sangster, M. J. Shoup III, C. Stoeckl, T. Thomas, and A. MacPhee, Rev.

This article is copyrighted as indicated in the article. Reuse of AIP content is subject to the terms at: http://scitation.aip.org/termsconditions. Downloaded to IP: 198.125.177.149 On: Wed, 04 Jun 2014 19:38:02

Sci. Instrum. **83**, 10E119 (2012); A. G. MacPhee, D. H. Edgell, E. J. Bond, D. K. Bradley, C. G. Brown, S. R. Burns, J. R. Celeste, C. J. Cerjan, M. J. Eckart, V. Y. Glebov, S. H. Glenzer, D. S. Hey, O. S. Jones, J. D. Kilkenny, J. R. Kimbrough, O. L. Landen, A. J. Mackinnon, N. B. Meezan, J. M. Parker and R. M. Sweeney, J. Instrum. **6**, P02009 (2011).

[37]S. F. Khan, P. M. Bell, D. K. Bradley, S. R. Burns, J. R. Celeste, L. S. Dauffy, M. J. Eckart, M. A. Gerhard, C. Hagmann, D. I. Headley, J. P. Holder, N. Izumi, M. C. Jones, J. W. Kellogg, H. Y. Khater, J. R. Kimbrough, A. G. Macphee, Y. P. Opachich, N. E. Palmer, R. B. Petre, J. L. Porter, R. T. Shelton, T. L. Thomas, and J. B. Worden, Proc. SPIE **8505**, 850505 (2012).

[38]L. M. Barker and R. E. Hollenbach, J. Appl. Phys. **43**, 4669 (1972).

[39]P. M. Celliers, D. K. Bradley, G. W. Collins, D. G. Hicks, T. R. Boehly, and W. J. Armstrong, Rev. Sci. Instrum. **75**, 4916 (2004).

[40]H. F. Robey, T. R. Boehly, P. M. Celliers, J. H. Eggert, D. Hicks, R. F. Smith, R. Collins, M. W. Bowers, K. G. Krauter, P. S. Datte, D. H. Munro, J. L. Milovich, O. S. Jones, P. A. Michel, C. A. Thomas, R. E. Olson, S. Pollaine, R. P. J. Town, S. Haan, D. Callahan, D. Clark, J. Edwards, J. L. Kline, S. Dixit, M. B. Schneider, E. L. Dewald, K. Widmann, J. D. Moody, T. Döppner, H. B. Radousky, A. Throop, D. Kalantar, P. DiNicola, A. Nikroo, J. J. Kroll, A. V. Hamza, J. B. Horner, S. D. Bhandarkar, E. Dzenitis, E. Alger, E. Giraldez, C. Castro, K. Moreno, C. Haynam, K. N. LaFortune, C. Widmayer, M. Shaw, K. Jancaitis, T. Parham, D. M. Holunga, C. F. Walters, B. Haid, E. R. Mapoles, J. Sater, C. R. Gibson, T. Mals- bury, J. Fair, D. Trummer, K. R. Coffee, B. Burr, L. V. Berzins, C. Choate, S. J. Brereton, S. Azevedo, H. Chandrasekaran, D. C. Eder, N. D. Masters, A. C. Fisher, P. A. Sterne, B. K. Young, O. L. Landen, B. M. Van Wonterghem, B. J. MacGowan, J. Atherton, J. D. Lindl, D. D. Meyerhofer, and E. Moses, Phys. Plasmas **19**, 042706 (2012).

[41]J. Frenje, R. Bionta, E. J. Bond, J. A. Caggiano, D. T. Casey, C. Cerjan, J. Edwards, M. Eckart, D. N. Fittinghoff, S. Friedrich, V. Yu. Glebov, S. Glenzer, G. Grim, S. Haan, R. Hatarik, S. Hatchett, M. Gatu Johnson, O. S. Jones, J. D. Kilkenny, J. P. Knauer, O. Landen, R. Leeper, S. Le Pape, R. Lerche, C. K. Li, A. Mackinnon, J. McNaney, F. E. Merrill, M. Moran, D. H. Munro, T. J. Murphy, R. D. Petrasso, R. Rygg, T. C. Sangster, F. H. Séguin, S. Sepke, B. Spears, P. Springer, C. Stoeckl, and D. C. Wilson, Nucl. Fusion **53**, 043014 (2013).

[42]J. Biener, D. D. Ho, C. Wild, E. Woerner, M. M. Biener, B. S. El-dasher, D. G. Hicks, J. H. Eggert, P. M. Celliers, G. W. Collins, N. E. Teslich, Jr., B. J. Kozioziemski, S. W. Haan, and A. V. Hamza, Nucl. Fusion **49**, 112001 (2009).

[43]G. A. Kyrala, J. L. Kline, S. Dixit, S. Glenzer, D. Kalantar, D. Bradley, N. Izumi, N. Meezan, O. Landen, D. Callahan, S. V. Weber, J. P. Holder, S. Glenn, M. J. Edwards, J. Koch, L. J. Suter, S. W. Haan, R. P. J. Town, P. Michel, O. Jones, S. Langer, J. D. Moody, E. L. Dewald, T. Ma, J. Ralph, A. Hamza, E. Dzenitis, and J. Kilkenny Phys. Plasmas **18**, 056307 (2011).

[44]S. H. Glenzer, B. K. Spears, M. J. Edwards, E. T. Alger, R. L. Berger, D. L. Bleuel, D. K. Bradley, J. A. Caggiano, D. A. Callahan, C. Castro, D. T. Casey, C. Choate, D. S. Clark, C. J. Cerjan, G. W. Collins, E. L. Dewald, J. G. Di Nicola, P. Di Nicola, L. Divol, S. N. Dixit, T. Doppner, R. Dylla-Spears, E. G. Dzenitis, J. E. Fair, L. J. A. Frenje, M. Gatu-Johnson, E. Giraldez, V. Glebov, S. M. Glenn, S. W. Haan, B. A. Hammel, S. P. Hatchett II, C. A. Haynam, R. F. Heeter, G. M. Heestand, H. W. Herrmann, D. G. Hicks, D. M. Holunga, J. B. Horner, H. Huang, N. Izumi, O. S. Jones, D. H. Kalantar, J. D. Kilkenny, R. K. Kirkwood, J. L. Kline, J. P. Knauer, B. Kozioziemski, A. L. Kritcher, J. J. Kroll, G. A. Kyrala, K. N. LaFortune, O. L. Landen, D. W. Larson, R. J. Leeper, S. Le Pape, J. D. Lindl, T. Ma, A. J. Mackinnon, A. G. MacPhee, E. Mapoles, P. W. McKenty, N. B. Meezan, P. Michel, J. L. Milovich, J. D. Moody, A. S. Moore, M. Moran, K. A. Moreno, D. H. Munro, B. R. Nathan, A. Nikroo, R. E. Olson, C. D. Orth, A. Pak, P. K. Patel, T. Parham, R. Petrasso, J. E. Ralph, H. Rinderknecht, S. P. Regan, H. F. Robey, J. S. Ross, J. D. Salmonson, C. Sangster, J. Sater, M. B. Schneider, F. H. Séguin, M. J. Shaw, M. J. Shoup, P. T. Springer, W. Stoeffl, L. J. Suter, C. A. Thomas, R. P. J. Town, C. Walters, S. V. Weber, P. J. Wegner, C. Widmayer, P. K. Whitman, K. Widmann, D. C. Wilson, B. M. Van Wonterghem, B. J. MacGowan, L. J. Atherton, and E. I. Moses, Plasma Phys. Controlled Fusion **54**, 045013 (2012).

This article is copyrighted as indicated in the article. Reuse of AIP content is subject to the terms at: http://scitation.aip.org/termsconditions. Downloaded to IP: 198.125.177.149 On: Wed, 04 Jun 2014 19:38:02